IEEE Access
Multidisciplinary | Rapid Review | Open Access Journal

Received June 20, 2018, accepted July 21, 2018, date of publication July 24, 2018, date of current version August 20, 2018.

*Digital Object Identifier 10.1109/ACCESS.2018.2859362*

# Doppler Power Spectra for 3D Vehicle-to-Vehicle Channels With Moving Scatterers

**XIAOLIN LIANG[1], WANGBIN CAO[2], AND XIONGWEN ZHAO[3], (Senior Member, IEEE)**

[1]School of Electronic and Information Engineering, Hebei University, Baoding 071002, China
[2]School of Electrical and Electronic Engineering, North China Electric Power University, Baoding 071000, China
[3]School of Electrical and Electronic Engineering, North China Electric Power University, Beijing 102206, China

Corresponding author: Wangbin Cao (wbin.cao@foxmail.com)

This work was supported in part by the Hebei University through the One Province One University Special Fund and in part by the Fundamental Research Funds for the Central Universities under Grant 2018MS096.

**ABSTRACT** A 3-D vehicle-to-vehicle (V2V) channel model composed by the line-of-sight, single-bounced and double-bounced rays with local scatterers moving in random velocities and directions is proposed in this paper. Based on the 3-D model, the complex channel gain and the autocorrelation function (ACF) are derived. The Doppler power spectral density (PSD) can be obtained by taking the Fourier transform to the ACF. As special cases, the proposed model can be applied to the 3-D fixed-to-vehicle (F2V) and fixed-to-fixed (F2F) scenarios at different carrier frequencies. The 2-D V2V, F2V, and F2F ACFs and Doppler PSDs can be obtained from the proposed 3-D model. Good agreements are shown between the theoretical and available measured Doppler PSDs in different scenarios in this paper.

**INDEX TERMS** Doppler power spectral density, single- and double- bounced, moving scatterers, 3-D channel, vehicle-to-vehicle.

## I. INTRODUCTION

Research on vehicle-to-vehicle (V2V) channel model and its characterization are of significance for the development and standardization of V2V communication system. Many different V2V channel models have been proposed in open literature, e.g. the regular-shaped geometry-based scattering models [1]–[5], the geometrical street models [6]–[8] and the geometrical T-junction models [9]. Narrowband channel measurements of the V2V channel and its characterization under realistic driving conditions have been reported in [10] and [11]. The measured Doppler delay profiles of wideband V2V channels can be found in [12] and [13]. The statistical properties of fixed-to-vehicle (F2V) [14], [15] and fixed-to-fixed (F2F) [16], [17] channels have been studied as the special cases for V2V channels. However, most these channel models just took the stationary scatterers into consideration, but the moving scatterers such as moving foliage, walking pedestrians and passing vehicles are inevitable in V2V communications, and the moving scatterers were proven to be a significant source for Doppler spread [18], even in millimeter wave band [19]. Most recently, some work took the moving scatterers into consideration. The Doppler spectrum of indoor channels considering moving scatterers was studied in [20] and [21]. The effect of moving scatterers on F2V and F2F channels was studied in [19] and [22], respectively. The geometrical street models in [7] and [8] investigated the statistics of the V2V channels with fixed and moving scatterers, but the velocities and directions of the moving scatterers were regarded as constant. A two-cylinder model for V2V channel with moving scatterers around the two bases of cylinders with constant velocities was proposed in [4]. A 2D V2V channel with single-bounced scatterering was proposed in [23], in which the scatterers were assumed to move with random velocities in random directions. However, in a V2V channel, apart from single-bounced (SB) rays, the LOS and double-bounced (DB) rays can also be happened frequently. Moreover, radio waves propagating in the elevation plane cannot be ignored, especially in a urban environment where the transmitter (Tx) and receiver (Rx) antennas are often located close to the ground and lower than the surroundings.

To overcome these aforementioned deficiencies, this paper proposes a 3D V2V channel model with local scatterers moving with random velocities in random directions, and it not only think about the single-bounced scattering rays but also the LOS and double-bounced rays are included in the model. The 3D complex channel gain and the autocorrelation functions (ACFs) of the LOS, SB and DB rays for V2V channel are derived. The corresponding 2D models can be obtained from the 3D model when the maximum elevation angle is set as zero degree. The ACFs of the F2V and F2F

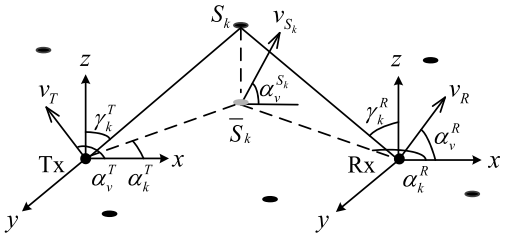


**FIGURE 1.** The 3D V2V SB scattering propagation scenario with moving scatterers.

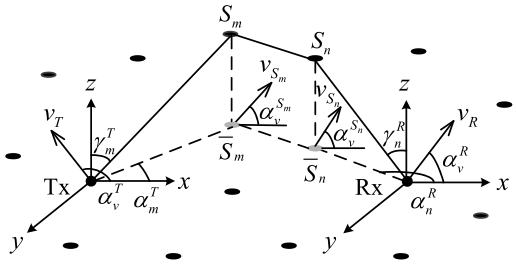


**FIGURE 2.** The 3D V2V DB scattering propagation scenario with moving scatterers.

channels can be derived as the special cases of the ACF for the V2V channel. The effect of different kind of local scatterers i.e., fixed scatterers, relatively slow and fast moving scatterers on the 2D/3D V2V, F2V and F2F channels are analyzed. It is assumed that the slow and fast moving scatterers follow negative exponential and Gaussian mixed distributions, respectively. The proposed 3D SB and DB scattering model are flexible to be applied to the regular geometrical models, such as one-sphere [24], two-cylinder [2] [models and so on. By considering the distributions of the angle-of-arrival (AoA) and angle-of-departure (AoD) of radio waves in one-sphere and two-cylinder models, the ACF and PSD of the two models are studied and compared with the measurement results.

The remainder of this paper is organized as follows. Section II presents the 3D geometrical LOS, SB and DB scattering model. Section III describes the autocorrelation function of the 3D V2V channel models. Section IV presents the numerical results and analysis. Section V summarizes the main findings and draws the conclusions.

## II. GEOMETRY OF THE SCATTERING MODEL

In this section, it is assumed that between the transceiver there may exist the line-of-sight (LOS), single-bounced (SB) and double-bounced (DB) scattering rays.

The geometry of the 3D V2V single-bounced scattering model is shown in Fig. 1. The transmitter (Tx) and receiver (Rx) are moving with the speed of $v_T$ and $v_R$, respectively. The angles $\alpha_v^T$ and $\alpha_v^R$ describe the moving orientations of the Tx and Rx in the x-y plane with respect to the x-axis. It is assumed that both the Tx and Rx are equipped with single omni-directional antennas. The Tx and Rx are surrounded by $K$ effect scatterers denoted by $S_k$ $(k = 1, 2, \ldots, K)$. The projection of the scatterer $S_k$ in the x-y plane is $\overline{S}_k$. Each of the local scatterers in motion with a random speed $v_{S_k}$ at a random direction $\alpha_v^{S_k}$. $\alpha_k^T$ and $\alpha_k^R$ denote the azimuth angles of departure (AAoD) and azimuth angles of arrival (AAoA) of the single-bounced rays, respectively. $\beta_k^T = \pi/2 - \gamma_k^T$ and $\beta_k^R = \pi/2 - \gamma_k^R$ denote the elevation angles of departure (EAoD) and elevation angles of arrive (EAoA) of the single-bounced rays, respectively. The AAoD $\alpha_k^T$ and AAoA $\alpha_k^R$, the EAoD $\beta_k^T$ and EAoA $\beta_k^R$ are dependent random variables.

The geometry of the 3D V2V double-bounced scattering model is shown in Fig. 2. The scatterers $S_m$ $(m = 1, 2, \ldots, M)$ and $S_n$ $(n = 1, 2, \ldots, N)$ move with random speeds $v_{S_m}$ and $v_{S_n}$ in random directions $\alpha_v^{S_m}$ and $\alpha_v^{S_n}$ in the x-y plane, respectively. The projections of the scatterers in the x-y plane are $\overline{S}_m$ and $\overline{S}_n$. $\alpha_m^T$ and $\alpha_n^R$ are the AAoD and AAoA of the double-bounced rays, respectively. $\beta_m^T = \pi/2 - \gamma_m^T$ and $\beta_n^R = \pi/2 - \gamma_n^R$ are the EAoD and EAoA of the double-bounced rays, respectively. The AAoD $\alpha_m^T$ and AAoA $\alpha_n^R$, the EAoD $\beta_m^T$ and EAoA $\beta_n^R$ are independent random variables.

The channel gain of frequency non-selective V2V SB and DB scattering models can be modeled as complex stochastic processes shown in (1) and (2), respectively.

$$\mu^{SB}(t) = \sum_{k=1}^{K} c_k e^{j(2\pi f_k t + \theta_k)} \tag{1}$$

$$\mu^{DB}(t) = \sum_{m=1}^{M}\sum_{n=1}^{N} c_{mn} e^{j(2\pi f_{mn} t + \theta_{mn})} \tag{2}$$

where $c_k$ and $c_{mn}$ designate the attenuation factor caused by the interaction of the emitted waves with the $k$-th scatterer $S_k$, the $m$-th scatterer $S_m$ and the $n$-th scatterer $S_n$, respectively. The random variables $\theta_k$ and $\theta_{mn}$ denote the phase shift and are assumed to be uniformly distributed between 0 and $2\pi$. $f_k$ and $f_{mn}$ represents the Doppler frequency caused by the movement of the transceiver and moving sactterers, respectively, which can be calculated as follows

$$\begin{aligned} f_k = \frac{k_0}{2\pi}[&v_T \cos(\alpha_k^T - \alpha_v^T)\cos\beta_k^T - v_{S_k}(\cos(\alpha_k^T - \alpha_v^{S_k}) \\ &\times \cos\beta_k^T + \cos(\alpha_v^{S_k} - \alpha_k^R)\cos\beta_k^R) \\ &+ v_R \cos(\alpha_k^R - \alpha_v^R)\cos\beta_k^R] \end{aligned} \tag{3}$$

$$\begin{aligned} f_{mn} = \frac{k_0}{2\pi}[&v_T \cos(\alpha_m^T - \alpha_v^T)\cos\beta_m^T - v_{S_m}(\cos(\alpha_m^T - \alpha_v^{S_m}) \\ &\times \cos\beta_m^T - \cos\alpha_v^{S_m}) - v_{S_n}(\cos(\alpha_v^{S_n} - \alpha_n^R)\cos\beta_n^R \\ &+ \cos\alpha_v^{S_n}) + v_R \cos(\alpha_n^R - \alpha_v^R)\cos\beta_n^R] \end{aligned} \tag{4}$$

where $k_0 = 2\pi f_0/c_0$ denotes the free-space wave number, $f_0$ is the carrier frequency, $c_0$ is the speed of light.

Based on the central limit theorem, if the number of paths tends to be infinity, the complex channel gain $\mu^{SB}(t)$ and $\mu^{DB}(t)$ in (1) and (2), respectively is equivalent to a complex valued Gaussian process with zero mean and variance $2\sigma_0^2(\lim_{K\to\infty}\sum_{k=1}^{K} E\{c_k^2\} = 2\sigma_0^2, \lim_{\substack{M\to\infty \\ N\to\infty}}\sum_{m=1}^{M}\sum_{n=1}^{N} E\{c_{mn}^2\} = 2\sigma_0^2)$, respectively.

The complex channel gain of the LOS rays are modeled as

$$\mu^{LOS}(t) = e^{j(2\pi f_{LOS}t+\theta_{LOS})} \tag{5}$$

where $f_{LOS}$ is the Doppler shift caused by the movement of the transceiver and can be calculated as

$$f_{LOS} = \frac{k_0}{2\pi}[v_T\cos(\pi - \alpha^R_{LOS} - \alpha^T_v) + v_R\cos(\alpha^R_{LOS} - \alpha^R_v)] \tag{6}$$

The AoAs are approximately equal to $\pi$ for the LOS rays, i.e., $\alpha^R_{LOS} = \pi$.

Then, the complex channel gain composing of LOS, single- and double- bounced rays can be modeled as

$$\mu(t) = \sqrt{\frac{K}{K+1}}\mu^{LOS}(t) + \sqrt{\frac{\eta^{SB}}{K+1}}\mu^{SB}(t) + \sqrt{\frac{\eta^{DB}}{K+1}}\mu^{DB}(t) \tag{7}$$

where $K$ is the Ricean factor, $\eta^{SB}$, $\eta^{DB}$ specify how much the SB and DB rays contribute in the total power and satisfy $\eta^{SB} + \eta^{DB} = 1$.

## III. AUTOCORRELATION FUNCTION OF THE 3D V2V CHANNEL MODELS

The ACF of the proposed single- and double- bounced models in Figs. 1 and 2 can be calculated by using the definition $r_{\mu\mu}(\tau) := E\{\mu^*(t)\mu(t+\tau)\}$, and $E\{\cdot\}$ denotes the expectation operator. Due to the wide applicability of the proposed model in (1) and (2), as long as the distributions of the AAoD, AAoA, EAoD and EAOA of the geometrical model are given, the ACF can be calculated.

### A. THE ACF OF THE PROPOSED MODEL

The ACF of the SB and DB rays can be obtained as (8) and (9) by substituting (1) and (2) into the definition of ACF, respectively.

$$r^{SB}_{\mu\mu}(\tau) = \lim_{K\to\infty}\sum_{k=1}^{K} c_k^2 E\{e^{j2\pi f_k\tau}\} \tag{8}$$

$$r^{DB}_{\mu\mu}(\tau) = \lim_{\substack{M\to\infty\\N\to\infty}}\sum_{m=1}^{M}\sum_{n=1}^{N} c_{mn}^2 E\{e^{j2\pi f_{mn}\tau}\} \tag{9}$$

It is assumed that all path gains have the same size, i.e., $c_k = \sigma_0\sqrt{2/K}$ and $c_{mn} = \sigma_0\sqrt{2/(MN)}$, for the SB and DB scattering rays, respectively. Under the assumption of isotropic scattering in azimuth plane, the AAoAs $\alpha^R_k$ and $\alpha^R_n$ of the SB and DB rays are uniformly distributed between 0 and $2\pi$. And the directions of moving scatterers $\alpha^{S_k}_v$, $\alpha^{S_m}_v$ and $\alpha^{S_n}_v$ are assumed to distribute uniformly in $(0, 2\pi]$. Then the ACF of the 3D V2V single- and double- bounced scattering rays can be obtained as (10) and (11), as shown at the top of the next page, respectively.

In (10), $p_{\alpha^T_k\alpha^R_k}(\alpha^T_k, \alpha^R_k)$ and $p_{\beta^T_k\beta^R_k}(\beta^T_k, \beta^R_k)$ describe the joint probability density function (pdf) of the AAoD and AAoA, as well as the EAoD and EAoA for the SB rays, respectively. In (11), $p_{\alpha^T_m}(\alpha^T_m)$ and $p_{\alpha^R_n}(\alpha^R_n)$ denote the pdf of the AAoD and AAoA for the DB rays, $p_{\beta^T_m}(\beta^T_m)$ and $p_{\beta^R_n}(\beta^R_n)$ denote the pdf of the EAoD and EAoA for the DB rays. $p_{\alpha^S_v}(\alpha^S_v)$ and $p_{v_S}(v_S)$ denote the pdf of the directions and velocities of moving scatterers, respectively.

If the AAoD $\alpha^T_k$ of SB rays are assumed to distribute uniformly in $[0, 2\pi]$, the ACF of the F2F channel ($v_T = v_R = 0$) for SB scattering with moving scaterers is simplified as expressed in (12), as shown at the top of the next page. If the scatterers are fixed ($v_{S_k} = v_{S_m} = v_{S_n} = 0$), the ACFs of the V2V channel can be simplified as (13), as shown at the top of the next page, where $J_0(\cdot)$ is the zero-order Bessel function of the first kind.

The ACF of the LOS rays can be calculated as

$$r^{LOS}_{\mu\mu}(\tau) = e^{j\frac{k_0}{2\pi}(v_T\cos\alpha^T_v - v_R\cos\alpha^R_v)\tau} \tag{14}$$

Since $\mu^{SB}(t)$ and $\mu^{DB}(t)$ are independent zero-mean complex Gaussian processes, the ACF of the channel gain $\mu(t)$ shown in (7) can be calculated as

$$r_{\mu\mu}(\tau) = \frac{K}{K+1}r^{LOS}_{\mu\mu}(\tau) + \frac{\eta^{SB}}{K+1}r^{SB}_{\mu\mu}(\tau) + \frac{\eta^{DB}}{K+1}r^{DB}_{\mu\mu}(\tau) \tag{15}$$

The pdf of EAoA $p_{\beta^R_k}(\beta^R_k)$ for SB rays, the pdfs of EAoD $p_{\beta^T_m}(\beta^T_m)$ and EAoA $p_{\beta^R_n}(\beta^R_n)$ for DB rays are expressed as in (16), which is prevalent in V2V communications [2].

$$p_\beta(\beta) = \begin{cases} \frac{\pi}{4|\beta_m|}\cos(\frac{\pi}{2}\frac{\beta}{\beta_m}), & |\beta| \le |\beta_m| \le \frac{\pi}{2} \\ 0, & \text{otherwise} \end{cases} \tag{16}$$

where $\beta_m$ is the maximum elevation angle.

### B. THE GEOMETRICAL SCATTERING MODEL

The one-sphere model can be obtained in [24]. For the SB rays, the relationships between the AAoD $\alpha^T_k$ and AAoA $\alpha^R_k$, the EAoD $\beta^T_k$ and EAoA $\beta^R_k$ are

$$\alpha^T_k \approx \frac{R_R}{D}\sin\alpha^R_k \tag{17}$$

$$\beta^T_k \approx \arccos(\frac{D + R_R\cos\beta^R_k\cos\alpha^R_k}{\xi_k}) \tag{18}$$

where $R_R$ is the radius of the Rx sphere, $D$ is the distance between the centers of the Tx and Rx, $\xi_k$ is the distance between the center of the Tx and the scatteter $S_k$.

The two-cylinder model is shown in [2]. For the SB rays, the relationships between the AAoD $\alpha^T_m$ and AAoA $\alpha^R_m$, the EAoD $\beta^T_m$ and EAoA $\beta^R_m$ impinged on scatterer $S_m$ around Tx are shown in (19) and (20), the relationships between the AAoD $\alpha^T_n$ and AAoA $\alpha^R_n$, the EAoD $\beta^T_n$ and EAoA $\beta^R_n$ impinged on scatterer $S_n$ around Rx are shown in (21) and (22).

$$\alpha^R_m \approx \pi - \frac{R_T}{D}\sin\alpha^T_m \tag{19}$$

$$\beta^R_m \approx \pi - (\frac{R_T}{D}\beta^T_m + \frac{h_T - h_R}{D}) \tag{20}$$

$$r_{\mu\mu}^{SB}(\tau) = 2\sigma_0^2 \int_{v_{S_k}} \int_{\beta_k^T} \int_{\beta_k^R} \int_{\alpha_k^T} \int_0^{2\pi} \int_0^{2\pi} e^{j\left[k_0 v_T \cos(\alpha_k^T - \alpha_v^T)\cos\beta_k^T - k_0 v_{S_k}(\cos(\alpha_k^T - \alpha_v^{S_k})\cos\beta_k^T + \cos(\alpha_v^{S_k} - \alpha_k^R)\cos\beta_k^R) + k_0 v_R \cos(\alpha_k^R - \alpha_v^R)\cos\beta_k^R\right]\tau}$$
$$\cdot p_{\alpha_v^{S_k}}\left(\alpha_v^{S_k}\right) \cdot p_{\alpha_k^T \alpha_k^R}\left(\alpha_k^T, \alpha_k^R\right) \cdot p_{\beta_k^T \beta_k^R}\left(\beta_k^T, \beta_k^R\right) \cdot p_{v_{S_k}}\left(v_{S_k}\right) d\alpha_v^{S_k} d\alpha_k^R d\alpha_k^T d\beta_k^T d\beta_k^R dv_{S_k} \tag{10}$$

$$r_{\mu\mu}^{DB}(\tau) = 2\sigma_0^2 \int_{v_{S_m}} \int_{\beta_m^T} \int_{\alpha_m^T} \int_0^{2\pi} e^{j\left[k_0 v_T \cos(\alpha_m^T - \alpha_v^T)\cos\beta_m^T - k_0 v_{S_m}(\cos\left(\alpha_m^T - \alpha_v^{S_m}\right)\cos\beta_m^T - \cos\alpha_v^{S_m})\right]\tau}$$
$$\cdot p_{\alpha_v^{S_m}}\left(\alpha_v^{S_m}\right) \cdot p_{\alpha_m^T}\left(\alpha_m^T\right) \cdot p_{\beta_m^T}\left(\beta_m^T\right) \cdot p_{v_{S_m}}\left(v_{S_m}\right) d\alpha_v^{S_m} d\alpha_m^T d\beta_m^T dv_{S_m}$$
$$\cdot \int_{v_{S_n}} \int_{\beta_n^R} \int_0^{2\pi} \int_0^{2\pi} e^{j\left[k_0 v_R \cos(\alpha_n^R - \alpha_v^R)\cos\beta_n^R - k_0 v_{S_n}(\cos\left(\alpha_v^{S_n} - \alpha_n^R\right)\cos\beta_n^R + \cos\alpha_v^{S_n})\right]\tau}$$
$$\cdot p_{\alpha_v^{S_n}}\left(\alpha_v^{S_n}\right) \cdot p_{\alpha_n^R}\left(\alpha_n^R\right) \cdot p_{\beta_n^R}\left(\beta_n^R\right) \cdot p_{v_{S_n}}\left(v_{S_n}\right) d\alpha_v^{S_n} d\alpha_n^R d\beta_n^R dv_{S_n} \tag{11}$$

$$r_{\mu\mu,\mathrm{F2F}}^{SB}(\tau) = \frac{\sigma_0^2}{\pi} \int_{v_{S_k}} \int_{\beta_k^T} \int_{\beta_k^R} \int_0^{2\pi} J_0(k_0 v_{S_k} \cos\beta_k^T \tau) \cdot J_0(k_0 v_{S_k} \cos\beta_k^R \tau) \cdot p_{\beta_k^T \beta_k^R}\left(\beta_k^T, \beta_k^R\right) \cdot p_{v_{S_k}}\left(v_{S_k}\right) d\alpha_v^{S_k} d\beta_k^T d\beta_k^R dv_{S_k} \tag{12}$$

$$r_{\mu\mu,\mathrm{V2V}}^{\text{fixed scatterers}}(\tau) = 2\sigma_0^2 \int_{\beta^T} J_0(k_0 v_T \cos\beta^T \tau) p_{\beta^T}\left(\beta^T\right) d\beta^T \cdot \int_{\beta^R} J_0(k_0 v_R \cos\beta^R \tau) \cdot p_{\beta^R}\left(\beta^R\right) \cdot d\beta^R \tag{13}$$

$$\alpha_n^T \approx \frac{R_R}{D} \sin\alpha_n^R \tag{21}$$

$$\beta_n^T \approx \frac{R_R}{D}\beta_n^R + \frac{h_T - h_R}{D} \tag{22}$$

where $R_T$ and $R_R$ are the radii of the Tx and Rx cylinders, $h_T$ and $h_R$ are the height of the Tx and Rx, $D$ is the distance between the centers of the Tx and Rx.

Assume the mathematical relation between AOD $\alpha^T$ and AOA $\alpha^R$ in a given geometric channel model is presented by $\alpha^T = g(\alpha^R)$, the joint pdf of $p_{\alpha^T\alpha^R}\left(\alpha^T, \alpha^R\right)$ of $\alpha^T$ and $\alpha^R$ can be expressed as [25]

$$p_{\alpha^T\alpha^R}\left(\alpha^T, \alpha^R\right) = p_{\alpha^R}\left(\alpha^R\right)\delta\left(\alpha^T - g\left(\alpha^R\right)\right) \tag{23}$$

The joint pdf of SB rays of the one-sphere and two-cylinder models can be obtained by Using (23).

### C. VELOCITY DISTRIBUTIONS OF MOVING SCATTERERS

The negative exponential distribution has been chosen to model the velocity of relatively slow moving scatterers [18], [19]. The negative exponential distribution can be expressed as (24), and $v_0$ is mean velocity.

$$p_{v_S}(v_S) = \begin{cases} \dfrac{1}{v_0}\exp(-\dfrac{v_s}{v_0}), & v_S \geq 0 \\ 0, & \text{otherwise} \end{cases} \tag{24}$$

The classical Gaussian and the Gauss mixed (GM) models [23] are the most popular probability distributions for describing the velocity of vehicles. The GM distribution can be expressed as

$$p_{v_S}(v_S) = \sum_{i=1}^{I} \omega_i N_i(v_S; m_{iv_S}, \sigma_{iv_S}^2) \tag{25}$$

where $\omega_i \geq 0$ is the mixing proportion, which is subject to $\sum_i \omega_i = 1$. The number of individual Gaussian densities $N_i$ is denoted by $I$, where each of them has mean $m_{iv_S}$ and variance $\sigma_{iv_S}^2$.

## IV. NUMERICAL RESULTS AND ANALYSIS

In the numerical calculation, the carrier frequency $f_0 = 5.9$GHz, the signal power $2\sigma_0^2$ is assumed to be 1. In the V2V channel, the velocity and moving directions of the Tx and the Rx are supposed to be $v^T = v^R = 20$km/h and $\alpha_v^T = \alpha_v^R = 0$, respectively. The negative exponential distribution (exp) is to describe the velocity of relatively slow moving scatterers [18] and the mean velocity is set as $m_{v_S} = 3.6$km/h in the exponential distribution. The Gaussian mixed (GM) distribution is to describe the velocity of relatively fast moving scatterers [23] and the GM parameters are set as: $I = 2$, $\omega_1 = \omega_2 = 0.5$, $m_{1v_S} = 20$km/h, $m_{2v_S} = 30$km/h, $\sigma_{1v_S} = \sigma_{2v_S} = 3.6$km/h. The EAoD and EAoA of the proposed SB and DB scattering models are assumed to follow the distribution in (16) and the maximum elevation angle is set to be $\beta_m = \pi/2$. In the one-sphere model, $R_R = 20$m, $D = 300$m. In the two-cylinder model, $R_T = R_R = 20$m, $D = 300$m. As the maximum elevation angle is set to 0, the 3D channel models are simplified to 2D models. The Doppler PSD can be calculated by taking the Fourier transform of the corresponding ACF.

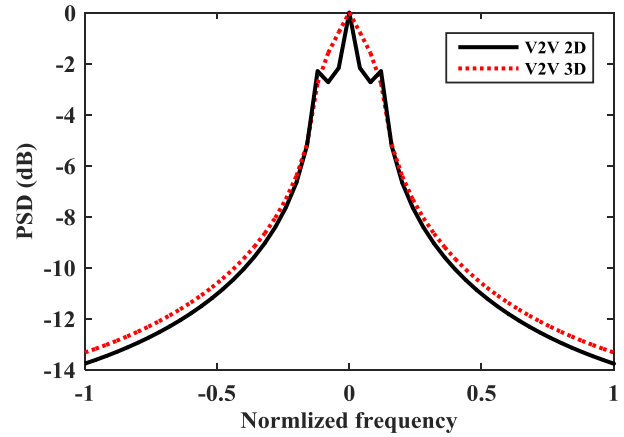


**FIGURE 3.** The Doppler PSDs of V2V channels with fixed scatterers.

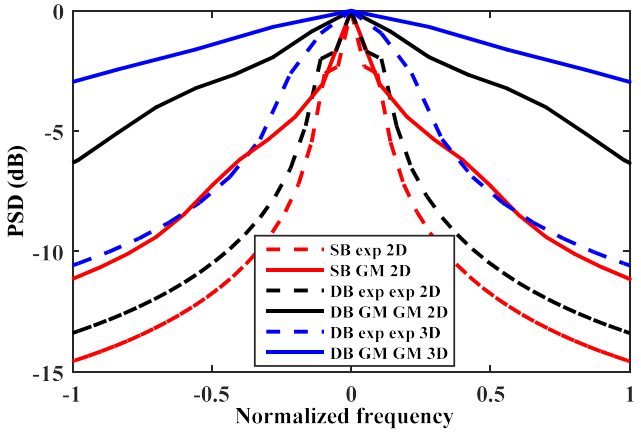


**FIGURE 4.** The Doppler PSDs of the SB and DB scattering V2V channels with moving scatterers.

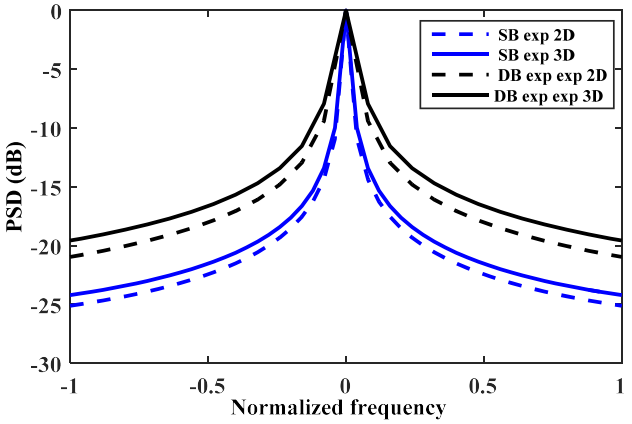


**FIGURE 5.** The Doppler PSDs of the SB and DB scattering F2F channels with slow moving scatterers.

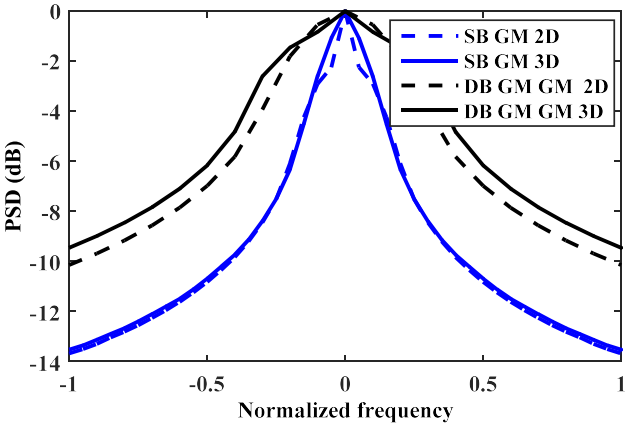


**FIGURE 6.** The Doppler PSDs of the SB and DB scattering F2F channels with fast moving scatterers.

### A. THE DOPPLER PSDS OF V2V CHANNELS WITH FIXED SCATTERERS

Fig. 3 shows the Doppler PSDs of V2V channels with fixed scatterers. The corresponding 2D V2V Doppler PSDs can be obtained when the maximum elevation angle is set to 0. It can be seen that the relative power of the 3D channels are different from the corresponding 2D one, i.e., the radio waves from elevation plane have obvious contribution to the Doppler PSDs of V2V channels with fixed scatterers. It is also seen that the Doppler spectra of the V2V channel are different from classical Jakes of the F2V channel.

### B. THE DOPPLER PSDS OF THE V2V CHANNEL WITH MOVING SCATTERERS

Fig. 4 shows the Doppler PSDs of single- and double-bounced rays of the V2V channel with relatively slow and fast moving scatterers, respectively. As shown in Fig. 4, no matter in 2D or 3D V2V models, the relative power is much higher by increasing the velocity of moving scatterers. And the power of the DB model is higher than that of the SB model, which means that the relative power can be increased with more scattering times. When the moving velocity or the number of scattering times increases, the Doppler spread becomes larger. We can also see that the relative power of the 3D model is larger than the 2D one for V2V channel with slow or fast moving scatterers.

### C. THE DOPPLER PSDS OF THE F2F CHANNEL WITH MOVING SCATTERERS

Figs. 5 and 6 show the Doppler PSDs of single- and double-bounced rays for the F2F channel with relatively slow and fast moving scatterers, respectively. From the two figures, it's seen that the Doppler PSDs of the DB scattering are with higher relative power than the SB scattering cases in both 2D and 3D F2F channels, i.e., by increasing number of the scattering times in the F2F channel, the Doppler spread becomes larger. And we can also see that the 3D Doppler PSDs is only slightly larger than 2D ones of the F2F channel for both SB and DB scattering, respectively with slow or fast moving scatterers.

### D. VALIDATION OF THE ANALYTICAL PSDs WITH MEASUREMENTS

Fig. 7 shows the analytical PSD of one-sphere model for 3D F2F channel with moving scatterers and the measured PSD for passing vehicles at 29.5GHz in [16]. In the numerical

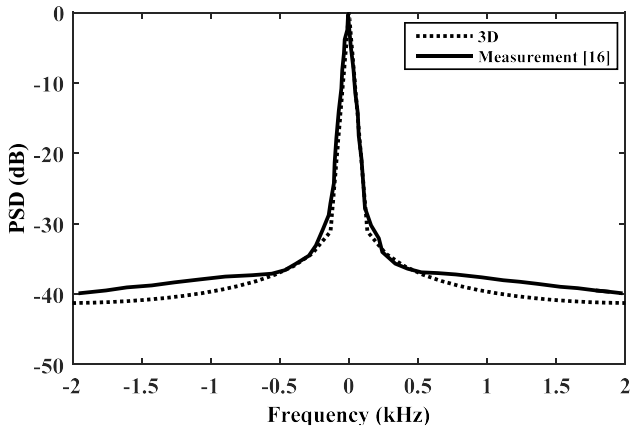


**FIGURE 7.** Comparison between the analytical PSD of 3D one-sphere model [24] and the measurement in [16].

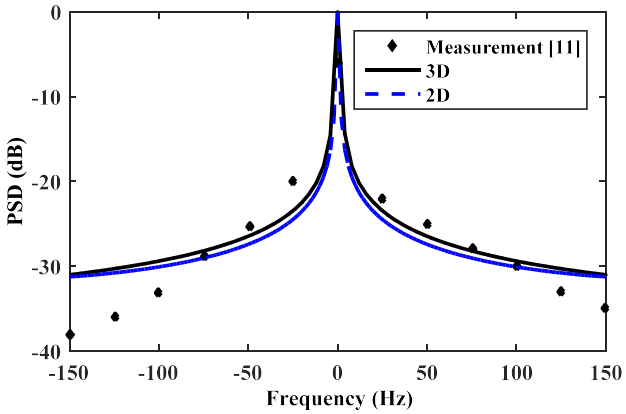


**FIGURE 8.** Comparison between the analytical 3D, 2D PSDs and measurement in [11].

computation, just the SB rays are considered. The pdfs of the AAoA, AAoD, EAoA and EAoD are assumed to follow the distributions as (17)(18). The GM distribution is used to describe the velocity distribution of moving scatterers, and the parameters are set as $\omega_1 = 0.4$, $m_{1v_S} = 20$km/h, $m_{2v_S} = 40$km/h, $\sigma_{1v_S} = \sigma_{2v_S} = 15$km/h [23] in the GM model. Very good agreement can be seen between the analytical and measured results.

Fig. 8 shows the analytical PSD of two-cylinder model for 3D V2V channel with fixed scatterers and the corresponding 2D model, as well as the measured result in [11]. In the two-cylinder model, we assume the 3D V2V channel is composed by the SB, DB and LOS rays and the parameters are taken as: $f_0 = 5.2$GHz, $f_T^{\max} = f_R^{\max} = 75$Hz, $\eta^{SBT} = \eta^{SBR} = 0.1$, $\eta^{DB} = 0.8$, and $K = 4$. The AAoD, AAOA, EAoD and EAoA of the SB and DB rays are assumed to follow the distributions as in (19)-(22). The 2D model is obtained by setting elevation angles as 0 in the 3D model. It is seen that the analytical result of 3D model matches better than the 2D model compared with the measurement.

## V. CONCLUSIONS

This paper proposes a 3D vehicle-to-vehicle (V2V) channel model where the local scatterers move with random velocities in random directions. In the channel model, the LOS, SB and DB scattering rays are taken into consideration. The negative exponential and Gaussian mixed distributions are used to describe the relatively slow and fast moving scatterers, respectively. The complex channel gain and autocorrelation function (ACF) of the channel model are derived and the Doppler power spectrum density (PSD) in different scenarios are analyzed. It can be found that the relative power in its PSD of the 3D models with fixed or moving scatterers for V2V or F2F channels are different from the corresponding 2D models. So the waves from the elevation plane cannot be ignored. It is also found that the Doppler PSDs and Doppler spread will become larger with the more scattering times or/and higher velocity of moving scatterers. The proposed model is flexible and can be applied for different regular geometrical models, e.g. one-sphere, two-cylinder and so on and it also can be applied at different carrier frequencies, even in the millimeter wave band. Good agreements can be found between the analytical Doppler PSDs in this work with the measurement results available so far.

## REFERENCES

[1] M. Pätzold, B. O. Hogstad, and N. Youssef, "Modeling, analysis, and simulation of MIMO mobile-to-mobile fading channels," *IEEE Trans. Wireless Commun.*, vol. 7, no. 2, pp. 510–520, Feb. 2008.

[2] A. G. Zajić and G. L. Stüber, "Three-dimensional modeling and simulation of wideband MIMO mobile-to-mobile channels," *IEEE Trans. Wireless Commun.*, vol. 8, no. 3, pp. 1260–1274, Mar. 2009.

[3] X. Cheng, C.-X. Wang, D. I. Laurenson, S. Salous, and A. V. Vasilakos, "An adaptive geometry-based stochastic model for non-isotropic MIMO mobile-to-mobile channels," *IEEE Trans. Wireless Commun.*, vol. 8, no. 9, pp. 4824–4835, Sep. 2009.

[4] A. G. Zajić, "Impact of moving scatterers on vehicle-to-vehicle narrow-band channel characteristics," *IEEE Trans. Veh. Technol.*, vol. 63, no. 7, pp. 3094–3106, Sep. 2014.

[5] Y. Yuan, C.-X. Wang, X. Cheng, B. Ai, and D. I. Laurenson, "Novel 3D geometry-based stochastic models for non-isotropic MIMO vehicle-to-vehicle channels," *IEEE Trans. Wireless Commun.*, vol. 13, no. 1, pp. 298–309, Jan. 2014.

[6] N. Avazov and M. Pätzold, "Design of wideband MIMO car-to-car channel models based on the geometrical street scattering model," *Model. Simul. Eng.*, vol. 2012, Sep. 2012, Art. no. 264213. [Online]. Available: https://www.hindawi.com/journals/mse/2012/264213/, doi: 10.1155/2012/264213.

[7] A. Chelli and M. Pätzold, "A non-stationary MIMO vehicle-to-vehicle channel model derived from the geometrical street model," in *Proc. IEEE VTC-Fall*, San Francisco, CA, USA, Sep. 2011, pp. 1–6.

[8] A. Chelli and M. Pätzold, "The impact of fixed and moving scatterers on the statistics of MIMO vehicle-to-vehicle channels," in *Radio Communications*, A. Bazzi, Ed. Vienna, Austria: InTech, 2010, ch. 3, pp. 51–63.

[9] H. Zhiyi, C. Wei, Z. Wei, M. Pätzold, and A. Chelli, "Modelling of MIMO vehicle-to-vehicle fading channels in T-junction scattering environments," in *Proc. 3rd EuCAP*, Berlin, Germany, Mar. 2009, pp. 652–656.

[10] L. Cheng, B. E. Henty, D. D. Stancil, F. Bai, and P. Mudalige, "Mobile vehicle-to-vehicle narrow-band channel measurement and characterization of the 5.9 GHz Dedicated Short Range Communication (DSRC) frequency band," *IEEE J. Sel. Areas Commun.*, vol. 25, no. 8, pp. 1501–1516, Oct. 2007.

[11] J. Maurer, T. Fügen, and W. Wiesbeck, "Narrow-band measurement and analysis of the inter-vehicle transmission channel at 5.2 GHz," in *Proc. 55th IEEE VTC-Spring*, Birmingham, AL, USA, vol. 3, May 2002, pp. 1274–1278.

[12] A. Paier *et al.*, "Car-to-car radio channel measurements at 5 GHz: Pathloss, power-delay profile, and delay-Doppler spectrum," in *Proc. Int. Symp. Wireless Commun. Syst. (ISWCS)*, Dec. 2007, pp. 224–228, doi: 10.1109/ISWCS.2007.4392335.

[13] Q. Wang, C. Xu, M. Wu, M. Zhao, and D. Yu, "Propagation characteristics of high speed railway radio channel based on broadband measurements at 2.6 GHz," in *Proc. IEEE WCNC*, Apr. 2014, pp. 166–170, doi: 10.1109/WCNC.2014.6951941.
[14] X. Zhao, J. Kivinen, P. Vainikainen, and K. Skog, "Characterization of Doppler spectra for mobile communications at 5.3 GHz," *IEEE Trans. Veh. Technol.*, vol. 52, no. 1, pp. 14–23, Jan. 2003.
[15] K. N. Le, "On angle-of-arrival and time-of-arrival statistics of geometric scattering channels," *IEEE Trans. Veh. Technol.*, vol. 58, no. 8, pp. 4257–4264, Oct. 2009.
[16] N. Naz and D. D. Falconer, "Temporal variations characterization for fixed wireless at 29.5 GHz," in *Proc. IEEE VTC*, Tokyo, Japan, May 2000, pp. 2178–2182.
[17] A. Domazetovic, L. J. Greenstein, N. B. Mandayam, and I. Seskar, "Estimating the Doppler spectrum of a short-range fixed wireless channel," *IEEE Commun. Lett.*, vol. 7, no. 5, pp. 227–229, May 2003.
[18] V.-H. Pham, M. H. Taieb, J.-Y. Chouinard, S. Roy, and H.-T. Huynh, "On the double Doppler effect generated by scatterer motion," *J. Electron. Commun.*, vol. 1, no. 1, pp. 30–37, Mar. 2011.
[19] S. Roy, H. T. Huynh, and P. Fortier, "Compound Doppler spread effects of subscriber motion and scatterer motion," *Int. J. Electron. Commun.*, vol. 57, no. 4, pp. 237–246, 2003.
[20] J. B. Andersen, J. O. Nielsen, G. F. Pedersen, G. Bauch, and G. Dietl, "Doppler spectrum from moving scatterers in a random environment," *IEEE Trans. Wireless Commun.*, vol. 8, no. 6, pp. 3270–3277, Jun. 2009.
[21] P. Pagani and P. Pajusco, "Characterization and modeling of temporal variations on an ultrawideband radio link," *IEEE Trans. Antennas Propag.*, vol. 54, no. 11, pp. 3198–3206, Nov. 2006.
[22] S. Thoen, L. van der Perre, and M. Engels, "Modeling the channel time-variance for fixed wireless communications," *IEEE Commun. Lett.*, vol. 6, no. 8, pp. 331–333, Aug. 2002.
[23] A. Borhani and M. Pätzold, "Correlation and spectral properties of vehicle-to-vehicle channels in the presence of moving scatterers," *IEEE Trans. Veh. Technol.*, vol. 62, no. 9, pp. 4228–4239, Nov. 2013.
[24] W. Chen, J. Zhang, Z. Liu, and Y. Bi, "A geometrical-based 3D model for fixed MIMO BS-RS channels," in *Proc. IEEE PIMRC*, Hongkong, Aug./Sep. 2015, pp. 502–506.
[25] S. Primak, V. Kontorovich, and V. Lyandres, *Stochastic Methods and Their Applications to Communications: Stochastic Differential Equations Approach*. Chichester, U.K.: Wiley, 2004.

**XIAOLIN LIANG** received the B.Sc. degree in electronic information technology from Hebei North University, China, in 2011, and the Ph.D. degree in electrical engineering & information technology from North China Electric Power University, Beijing, China, in 2017. She has been with the School of Electronic and Information Engineering, Hebei University, Since 2017. Her main research interests include multiple-input multiple-output (MIMO) mobile-to-mobile/ vehicle-to vehicle / device-to-device communications, millimeter wave communications, antennas and diversity techniques, and advanced wireless MIMO channel modeling and simulation.

**WANGBIN CAO** was born in Dingxi, Gansu, China. He received the B.Eng. degree in electronic information & science technology from the School of Electrical & Electronic Engineering, North China Electric Power University (NCEPU), in 2011, the master's degree in communication & information system from NCEPU in 2013, and the Ph.D. degree in electrical information & engineering technology from the School of Electrical and Electronic Engineering, NCEPU, Beijing, China, in 2017. He was with NCEPU, Baoding, China, from 2007 to 2011. He is currently a Lecturer with the School of Electrical and Electronic Engineering, NCEPU, where he is currently focusing on the research of MIMO communications and intelligent power distribution.

**XIONGWEN ZHAO** (SM'06) was born in Qingjian, Shanxi, China, in 1964. He received the Ph.D. degree (Hons.) from the Helsinki University of Technology (TKK), Finland, in 2002. From 1992 to 1998, he was with the Laboratory of Communications System Engineering, China Research Institute of Radiowave Propagation, where he was the Director and a Senior Engineer. From 1999 to 2004, he was with the Radio Laboratory, TKK, as s Senior Researcher and a Project Manager in the areas of MIMO channel modeling and measurements at 2, 5, and 60GHz as well as UWB. From 2004 to 2011, he was with Elektrobit Corporation (EB), Espoo, Finland, as a Senior Specialist at EB wireless solutions. From 2004 to 2007, he involved in the European WINNER project as a Senior Researcher in MIMO channel modeling for 4G radio systems. From 2006 to 2008, he also involved in the field of wireless network technologies such as WiMAX and wireless mesh networks. From 2008 to 2009, he involved in satellite mobile communications for GMR-1 3G, DVB-SH RF link budget, and antenna performance evaluations. From 2010 to 2011, he involved in the spectrum sharing and interference management between satellite and terrestrial LTE networks. He is currently a Professor in wireless communications with North China Electric Power University, Beijing, chairs a project supported by the National Science Foundation of China, and participates a National 863 Project on 5G networks. He has served as the TPC Member for numerous IEEE Conferences. He was a recipient of the IEEE Vehicular Technology Society Neal Shepherd Best Propagation Paper Award in 2014. He is a reviewer of the IEEE TRANSACTIONS, Journals, Letters, and Conferences. His IEEE publications on mobile channel models have been cited over 1000 times worldwide.